J. Fluid Mech. (1974), *vol.* 65, *part* 3, *pp.* 481–498
Printed in Great Britain

A laminar boundary layer on a rotating three-dimensional blade

By Y. MIYAKE AND S. FUJITA†
Department of Mechanical Engineering, Osaka University, Osaka, Japan

(Received 18 September 1973)

The laminar boundary layer on a rotating thin blade of an axial turbomachine is discussed. A method of deriving the basic equations of the flow for a generalized blade configuration is described, treating a typical blade in practical use as an example. A perturbation technique is applied to obtain a series solution composed of two groups of similar functions. The results give insight into the properties of the boundary layer on helical non-loaded blades in a uniform stream, indicating the influence purely of three-dimensionality of the blade configuration.

1. Introduction

The laminar boundary layer on a rotating blade such as a rotor blade of an axial turbomachine or a helicopter rotor was first studied by Fogarty (1951) and further detailed studies have been performed by many authors in the last decade. Fogarty approximated the rotating blade by a flat plate which rotates in its plane about an axis perpendicular to its leading edge and gave a solution which is valid in the region far from the axis of rotation. Generally, this boundary-layer flow is three-dimensional because of the centrifugal force due to rotation, but in Fogarty's solution, the so-called independence principle holds with regard to the spanwise and the chordwise flow. Tan (1953) extended Fogarty's work and presented a series solution which is valid in a region nearer to the axis of rotation.

Bogdanova (1971) and Takematsu (1972) studied the case of an aerofoil blade of finite thickness. Toyokura & Harada (1969) made an approximate analysis by means of integral equations including the case of a turbulent boundary layer. Furthermore, McCrosky & Yaggy (1968) treated the case of a helicopter rotor with translational and hovering motion. However, in all these studies the analysis is simplified by the assumption that the blades are two-dimensional.

The rotor blade of an axial turbomachine is generally twisted so that the angle of attack has a specified value which varies in the spanwise direction. Horlock & Wordsworth (1965) analysed the laminar boundary layer on a thin helical blade whose blade angle, or the inclination of a blade element to the axial flow direction, is constant everywhere on the blade surface, although the blade is three-dimensional. They could formulate successfully the effect of stagger on the laminar boundary layer, but the effect of twist, namely, the effect of spanwise variation of the blade angle, could not be taken into account.

† Present address: Mitsubishi Heavy Industry Co. Ltd, Kobe, Japan.

The present analysis deals with the laminar boundary layer on a rotating blade which is twisted with the centre of twist at the leading edge, so that the angle of attack becomes zero everywhere at the leading edge. The blade is assumed to be infinitely long and the effect of the hub and casing walls on the boundary-layer flow is not taken into account.

2. Blade configuration and co-ordinate systems

Consider a thin blade with a straight leading edge which rotates in a uniform stream U with angular velocity ω as illustrated in figure 1. Take a right-handed rectilinear co-ordinate system ξ_i fixed to the leading edge in which the ξ_2 and ξ_3 axes are the axis of rotation and the leading edge, respectively. In this paper all the vector components having subscripts represent covariant components and those with superscripts contravariant ones. To avoid confusion, any quantity A raised to the power n will be denoted by $(A)^n$.

Many kinds of blade configuration meet the condition that the angle of attack becomes zero along the leading edge. This paper adopts the configuration which is specified by the curved surface defined by the following equations:

$$\xi_1 = x_1 \cos\phi, \quad \xi_2 = x_1 \sin\phi, \quad \xi_3 = x_3, \tag{1}$$

$$\tan\phi = U/\omega x_3, \tag{2}$$

in which x_3 and ξ_3 have the same origin and the origin of x_1 lies on the leading edge, namely, on the ξ_3 axis. Equation (2) is derived from consideration of a velocity triangle at the leading edge. The angle ϕ is the angle between the uniform approaching flow and a straight line $x_3 =$ constant on the blade surface. Take the third co-ordinate axis x_2 perpendicular to the x_1 and x_3 axes such that they constitute a right-handed system. On the blade surface, the x_2 axis is coincident with the normal to the blade surface. In the limiting case $x_3 = 0$, the blade element lies on the ξ_2 axis or on the axis of rotation and in the other limiting case $x_3 \to \infty$, or sufficiently far from the axis of rotation, the blade becomes a flat plate.

The direction cosines of a line $x_1 =$ constant on the blade surface are

$$l_3 = x_1 \sin^2\phi \cos\phi/S, \quad m_3 = -x_1 \sin\phi \cos^2\phi/S, \quad n_3 = x_3/S, \tag{3}$$

where $S = \{(x_3)^2 + (x_1)^2 \sin^2\phi \cos^2\phi\}^{\frac{1}{2}}$. Those for a line $x_3 =$ constant on the blade surface are

$$l_1 = \cos\phi, \quad m_1 = \sin\phi, \quad n_1 = 0. \tag{4}$$

From (3) and (4), one has $l_1 l_3 + m_1 m_3 + n_1 n_3 = 0$, which means that the lines of constant x_1 and x_3 form an orthogonal curvilinear mesh on the blade surface.

The direction cosines of the x_2 axis are

$$l_2 = -x_3 \sin\phi/S, \quad m_2 = x_2 \cos\phi/S, \quad n_2 = x_1 \sin\phi \cos\phi/S. \tag{5}$$

An arbitrary point in space expressed in ξ_i co-ordinates is given in x_i curvilinear co-ordinates by using these relations as

$$\xi_1 = x_1 \cos\phi + x_2 l_2, \quad \xi_2 = x_1 \sin\phi + x_2 m_2, \quad \xi_3 = x_3 + x_2 n_2. \tag{6}$$

This curvilinear co-ordinate system is orthogonal on the blade surface, but not at any point detached from the surface. Covariant base vectors are taken in the directions of the positive x_i axes and one can calculate the metric tensor for the x_i co-ordinate system from (6). The set of covariant components is

$$\left.\begin{aligned} &g_{11} = 1+O\{(x_2)^2\}, \quad g_{12} = g_{21} = 0, \quad g_{13} = g_{31} = 2x_2 \sin\phi\cos\phi/S + O\{(x_2)^2\},\\ &g_{32} = g_{23} = 0, \quad g_{22} = 1,\\ &g_{33} = 1+(x_1/x_3)^2\sin^2\phi\cos^2\phi - 4(x_1/x_3)\,x_2\sin\phi\cos^3\phi/S + O\{(x_2)^2\} \end{aligned}\right\} \tag{7}$$

and that of contravariant components is

$$\left.\begin{aligned} &g^{11} = 1+O\{(x_2)^2\}, \quad g^{12} = g^{21} = 0,\\ &g^{13} = g^{31} = 2x_2(x_3)^2\sin\phi\cos\phi/(S)^3 + O\{(x_2)^2\}, \quad g^{22} = 1,\\ &g^{33} = (x_3)^2/(S)^2 + 4x_1x_2(x_3)^3\sin\phi\cos^3\phi/(S)^5 + O\{(x_2)^2\}, \end{aligned}\right\} \tag{8}$$

where $O\{(x_2)^2\}$ means the small terms of order smaller than $(x_2)^2$, x_2 being considered to be small in the framework of boundary-layer theory. The Christoffel functions of the first kind $\Gamma_{k,ij}$ and the second kind Γ^i_{jk} are calculated from (7) and (8). The Γ^i_{jk} are as follows:

$$\left.\begin{aligned} &\Gamma^1_{11} = \Gamma^1_{12} = \Gamma^1_{13} = \Gamma^1_{21} = \Gamma^1_{31} = \Gamma^3_{11} = \Gamma^2_{11} = O(x_2),\\ &\Gamma^1_{22} = \Gamma^2_{12} = \Gamma^2_{21} = \Gamma^2_{22} = \Gamma^2_{23} = \Gamma^2_{32} = \Gamma^3_{22} = 0,\\ &\Gamma^1_{23} = \Gamma^1_{32} = \sin\phi\cos\phi/S + O(x_2),\\ &\Gamma^1_{33} = -\{x_1/(x_3)^2\}\sin^2\phi\cos^2\phi + O(x_2),\\ &\Gamma^2_{13} = \Gamma^2_{31} = -\sin\phi\cos\phi/S + O(x_2),\\ &\Gamma^2_{33} = 2(x_1/x_3)\sin\phi\cos^3\phi/S + O(x_2),\\ &\Gamma^3_{12} = \Gamma^3_{21} = -(x_3)^2\sin\phi\cos\phi/(S)^3 + O(x_2),\\ &\Gamma^3_{13} = \Gamma^3_{31} = -x_1\sin^2\phi\cos^2\phi/(S)^2 + O(x_2),\\ &\Gamma^3_{23} = \Gamma^3_{32} = -2x_1x_3\sin\phi\cos^3\phi/(S)^3 + O(x_2),\\ &\Gamma^3_{33} = 4\{(x_1)^2/x_3\}\sin^4\phi\cos^4\phi/(S)^2 + O(x_2). \end{aligned}\right\} \tag{9}$$

3. Equation of motion and equation of continuity

The equation of motion of incompressible flow relative to a rotating co-ordinate system whose angular velocity is $\boldsymbol{\omega}$ is, in vector form,

$$\nabla(p/\rho + \tfrac{1}{2}(w)^2 - \tfrac{1}{2}(r\omega)^2) + \nabla\times\mathbf{w}\times\mathbf{w} = -\nu\nabla\times(\nabla\times\mathbf{w}) - 2\boldsymbol{\omega}\times\mathbf{w}, \tag{10}$$

where $\mathbf{w}$ is the relative velocity vector, of magnitude w, r the distance from the axis of rotation, p the static pressure and ρ and ν the density and kinematic viscosity, respectively. The tensor expression in contravariant form of (10) can be obtained by taking components of each term of (10) in the direction of the covariant base vector $\mathbf{g}_i$. It is

$$w^j w^i_{,j} = -\frac{g^{ij}}{\rho}\frac{\partial p}{\partial x_j} + \nu g^{jk} w^i_{,jk} - 2\epsilon^{rsi}\omega_r w_s + \frac{g^{ij}}{2}(\omega)^2\frac{\partial(r)^2}{\partial x_j}, \tag{11}$$

where

$$(r)^2 = (x_1)^2\cos^2\phi + (x_3)^2 + (x_2)^2\,(x_3)^2/(S)^2,$$

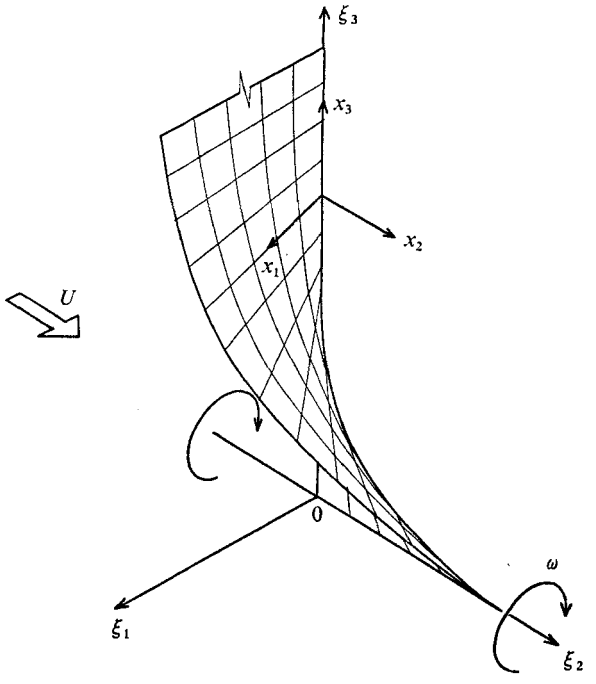

FIGURE 1. Blade configuration and co-ordinate systems.

and e^{rsi} is the permutation tensor, the w^i are contravariant relative velocities which are related to the physical components $\hat{w}_i$ according to

$$w^i = \hat{w}_i/\sqrt{g_{ii}} \quad \text{(no summation convention)} \tag{12}$$

and $w^i_{,j}$ is the covariant differential of w^i defined by

$$w^i_{,j} = \partial w^i/\partial x_j + \Gamma^i_{jk} w^k. \tag{13}$$

ω_r in (11) is related to the rectilinear components ω^*_k of $\boldsymbol{\omega}$ by

$$\omega_r = \boldsymbol{\omega} \,.\, \mathbf{g}_r = \omega^*_k(\partial \xi^k/\partial x_r),$$

and the ω^*_k are, owing to the definition of the ξ_i co-ordinate system, given by

$$\omega^*_1 = 0, \quad \omega^*_2 = -\omega, \quad \omega_3 = 0. \tag{14}$$

The covariant components w_r in (11) can be obtained in terms of the w^j as

$$w_r = g_{rj} w^j.$$

Whence (11) is regarded as the equation of motion for the contravariant relative velocities w^j.

The tensor expression for the equation of continuity $\nabla \,.\, \mathbf{w} = 0$ is

$$w^i_{,i} = 0 \quad \text{or} \quad \partial(g^{\frac{1}{2}} w^i)/\partial x_i = 0, \tag{15}$$

where $$g = |g_{ij}| = \{1 + (x_1/x_3)^2 \sin^2\phi \cos^2\phi\} + O(x_2).$$

4. Boundary-layer equations

The usual boundary-layer approximation is carried out for (11) and (15), assuming that the Reynolds number is sufficiently large. Γ^i_{jk} which appear in the scalar form of those equations are expanded in power series in x_2. The terms in $(x_2)^0$ are retained, being of order of magnitude unity, and all other terms are omitted. The resulting boundary-layer equations are, after a little laborious calculation,

$$\left.\begin{aligned} w^1\frac{\partial w^1}{\partial x_1}+w^2\frac{\partial w^1}{\partial x_2}+w^3\frac{\partial w^1}{\partial x_3}+2\Gamma^1_{33}-2\omega w^3\cos\phi-x_1(\omega)^2\cos^2\phi& \\ =-\frac{1}{\rho}g^{11}\frac{\partial p}{\partial x_1}+\nu\frac{\partial^2 w^1}{\partial x_2\partial x_2},& \\ w^1\frac{\partial w^3}{\partial x_1}+w^2\frac{\partial w^3}{\partial x_2}+w^3\frac{\partial w^3}{\partial x_3}+2\Gamma^3_{33}w^3w^3+2\Gamma^3_{13}w^1w^3& \\ +\frac{2\omega(x_3)^2w^1\cos\phi}{\{(x_3)^2+(x_1)^2\sin^2\phi\cos^2\phi\}}-x_3(\omega)^2=-\frac{g^{33}}{\rho}\frac{\partial p}{\partial x_3}+\nu\frac{\partial^2 w^3}{\partial x_2\partial x_2},& \\ \partial p/\partial x_2=0,& \end{aligned}\right\} \tag{16}$$

where Γ^1_{33}, Γ^3_{33}, Γ^3_{13}, g^{11} and g^{33} are given by (8) and (9) with the higher-order infinitesimal terms omitted. Similarly, the equation of continuity becomes

$$\frac{\partial w^1}{\partial x_1}+\frac{\partial w^2}{\partial x_2}+\frac{\partial w^3}{\partial x_3}=-\frac{x_1\sin^2\phi\cos^2\phi\,(w^1x_3-2w^3x_1\cos^2\phi)}{x_3\{(x_3)^2+(x_1)^2\sin^2\phi\cos^2\phi\}}. \tag{17}$$

In the limit $x_3\to\infty$, $\phi\to 0$, and (16) and (17) become

$$\left.\begin{aligned} w^1\frac{\partial w^1}{\partial x_1}+w^2\frac{\partial w^1}{\partial x_2}+w^3\frac{\partial w^1}{\partial x_3}-2\omega w^3-x_1(\omega)^2=-\frac{1}{\rho}\frac{\partial p}{\partial x_1}+\nu\frac{\partial^2 w^1}{\partial x_2\partial x_2},& \\ w^1\frac{\partial w^3}{\partial x_1}+w^2\frac{\partial w^3}{\partial x_2}+w^3\frac{\partial w^3}{\partial x_3}+2\omega w^1-x_3(\omega)^2=-\frac{1}{\rho}\frac{\partial p}{\partial x_3}+\nu\frac{\partial^2 w^3}{\partial x_2\partial x_2},& \\ \frac{\partial p}{\partial x^2}=0,\quad \frac{\partial w^1}{\partial x_1}+\frac{\partial w^2}{\partial x_2}+\frac{\partial w^3}{\partial x_3}=0.& \end{aligned}\right\} \tag{18}$$

Solution of these equations gives the contravariant velocities, but these velocities are coincident with the physical ones in the limit $\phi\to 0$, since $g^{11}\to 1$ and $g^{33}\to 1$ then. Equations (18) may also be obtained simply by putting $\phi=0$ in (16) and (17), and are the fundamental equations that all the previous authors except for Horlock & Wordsworth used as the starting point of the analysis. The problem considered in the present analysis is a more general case which includes the case $\phi=0$ as a special one, and the solution for $\phi=0$ is obtained easily from the solution given below simply by putting $\beta=0$, β being the parameter representing the three-dimensionality of the blade contained in the solution. The above-mentioned technique is applicable for any other blade configuration if one is ready to handle the slightly more complicated mathematics which arise from the non-orthogonality of the curvilinear co-ordinate system.

5. The mainstream flow

Equations (16) and (17) can be solved with any kind of mainstream flow in principle. In general, pressure variation along a blade element is determined by the mainstream potential flow. However, for the purposes of the present analysis, it is advantageous to adopt as simple a flow as possible. In this study, it is assumed that each streamline is the intersection of the blade surface and a circular cylinder whose centre-line is at the axis of rotation and that the magnitude of the velocity is constant. This mainstream flow is, in an exact sense, a hypothetical one and the blade is slightly loaded. To analyse the effect purely of three-dimensionality of a blade, the best way may be to adopt a helical blade with constant velocity along a blade element and with the pressure constant everywhere in the flow field. But the difference between this ideal case and the present one manifests itself in terms smaller than $(x_1/x_3)^4$ of the series solution given below.

Now, the streamlines can be specified as

$$\left.\begin{aligned} &\xi_1 = x_1\cos\phi, \quad \xi_2 = x_1\sin\phi, \quad \xi_3 = x_3, \\ &(\xi_1)^2+(\xi_3)^2 = \text{constant}, \quad \tan\phi = U/\omega x_3, \end{aligned}\right\} \tag{19}$$

which defines a three-dimensional curve, the direction cosines of which relative to the ξ_i axes are

$$l_T = -(x_3)^2\cos\phi/T, \quad m_T = -\sin\phi\{(x_3)^2+(x_1)^2\cos^2\phi\}/T, \quad n_T = x_1x_3\cos^2\phi/T, \tag{20}$$

where $$T = \{(x_3)^4+(x_1)^4\sin^2\phi\cos^4\phi+(x_1)^2(x_3)^2\cos^2\phi(1+\sin^2\phi)\}^{\frac{1}{2}}.$$

The magnitude $\hat{W}$ of the velocity of the mainstream flow is constant as is assumed above, and is given by

$$\hat{W} = \{(U)^2+(r\omega)^2\}^{\frac{1}{2}} = [(\omega)^2\{(x_1)^2\cos^2\phi+(x_3)^2\}+(U)^2]^{\frac{1}{2}}. \tag{21}$$

The physical components $\hat{W}_i$ in the x_i directions are calculated to be

$$\hat{W}_1 = \hat{W}(l_1l_T+m_1m_T+n_1n_T), \quad \hat{W}_2 = 0, \quad \hat{W}_3 = \hat{W}(l_3l_T+m_3m_T+n_3n_T),$$

and may be transformed into the contravariant components W^i according to (12):

$$\left.\begin{aligned} W^1 &= \{(x_3)^2+(x_1)^2\sin^2\phi\cos^2\phi\} \\ &\quad\times\left[\frac{(\omega)^2\{(x_1)^2\cos^2\phi+(x_3)^2\}+(U)^2}{(x_3)^4+(x_1)^4\sin^2\phi\cos^4\phi+(x_1)^2(x_3)^2\cos^2\phi(1+\sin^2\phi)}\right]^{\frac{1}{2}}, \\ W^2 &= 0, \\ W^3 &= -x_1x_3\left[\frac{(\omega)^2\{(x_1)^2\cos^2\phi+(x_3)^2\}+(U)^2}{(x_3)^4+(x_1)^4\sin^2\phi\cos^4\phi+(x_1)^2(x_3)^2\cos^2\phi(1+\sin^2\phi)}\right]^{\frac{1}{2}}. \end{aligned}\right\} \tag{22}$$

The equation of motion that these velocities satisfy is obtained by neglecting viscous terms and putting $x_2 = 0$ and $w^i = W^i$ in (16). This gives

$$\left.\begin{aligned} &W^1\frac{\partial W^1}{\partial x_1}+W^3\frac{\partial W^1}{\partial x_3}+2\Gamma^1_{33}W^3W^3-2\omega W^3\cos\phi-x_1(\omega)^2\cos\phi = -\frac{g^{11}}{\rho}\frac{\partial p}{\partial x_1}, \\ &W^1\frac{\partial W^3}{\partial x_1}+W^3\frac{\partial W^3}{\partial x_3}+2\Gamma^3_{33}W^3W^3+2\Gamma^3_{13}W^1W^3+\frac{2\omega W^1(x_3)^2\cos\phi}{(x_3)^2+(x_1)^2\sin^2\phi\cos^2\phi}, \\ &\qquad -(\omega)^2x_3 = (-g^{33}/\rho)\,\partial p/\partial x_3, \end{aligned}\right\} \tag{23}$$

which enables one to eliminate the pressure term and the centrifugal term in (16).

The boundary conditions for (16) and (17) are obtained from the no-slip condition at the wall and matching w^i with W^i at $x_2 \to \infty$, and are as follows:

$$\left.\begin{aligned} w^1 = w^2 = w^3 = 0 \quad &\text{at} \quad x_2 = 0, \\ w^1 \to W^1, \quad w^3 \to W^3 \quad &\text{as} \quad x_2 \to \infty. \end{aligned}\right\} \tag{24}$$

6. The solution of the boundary-layer equation

Let the characteristic lengths in the x_1 and x_3 directions be c and L respectively and consider the case where $\epsilon \equiv c/L \ll 1$. In the limit $\epsilon \to 0$, $W^1 \sim x_1\omega$ and $W^3 \sim x_3\omega$, so that, taking ϵ as the perturbation parameter, one can expect a solution of the form

$$\frac{w^1}{x_3\omega} = \sum_{k=0}^{\infty} w^1_{(k)} = \sum_{k=0}^{\infty} \left(\frac{x_1}{x_3}\right)^k \tilde{w}^1_{(k)}, \quad \frac{w^3}{x_3\omega} = \sum_{k=1}^{\infty} w^3_{(k)} = \sum_{k=1}^{\infty} \left(\frac{x_1}{x_3}\right)^k \tilde{w}^3_{(k)}. \tag{25}$$

As for w^2, the expansion

$$\frac{w^2}{x_3\omega} = \sum_{k=0}^{\infty} w^2_{(k)} = \sum_{k=0}^{\infty} \left(\frac{\nu x_1}{\omega x_3}\right)^{\frac{1}{2}} \left(\frac{x_1}{x_3}\right)^k \tilde{w}^2_{(k)} \tag{26}$$

is possible, since $w^2 \sim (\delta/c)w^1$, δ being the thickness of the boundary layer, whose order of magnitude is $\delta \sim (c\nu/L\omega)^{\frac{1}{2}}$. In the expansion given above, the $\tilde{w}^i_{(k)}$ are of order one and $w^1_{(k)}$, $w^2_{(k)}$ and $w^3_{(k)}$ are of order ϵ^k, $\delta\epsilon^k$ and ϵ^k respectively. The components of the metric tensor and other terms concerning the mainstream flow are also expanded in power series in x_1/x_3. Introducing a non-dimensional length $\tilde{x}_i$ of order one, defined as

$$x_1 = c\tilde{x}_1, \quad x_2 = c\delta\tilde{x}_2, \quad x_3 = L\tilde{x}_3,$$

quantities such as, say, $\cos\phi$ are expanded as

$$\cos\phi = 1 - \tfrac{1}{2}\epsilon^2(\kappa/\tilde{x}_3)^2 + \tfrac{3}{8}\epsilon^4(\kappa/\tilde{x}_3)^4 + \ldots, \quad \kappa = U/\omega c.$$

All these series are substituted into (16) and (17). Collecting the terms in ϵ^k, one finds that the order-k velocities must satisfy the following equations:

$$\left.\begin{aligned} \sum_{m=0}^{k} \left\{ w^1_{(m)} \frac{\partial w^1_{(k-m)}}{\partial x_1} + w^2_{(m)} \frac{\partial w^1_{(k-m)}}{\partial x_2} + w^3_{(m)} \frac{\partial w^1_{(k-m)}}{\partial x_3} \right\} &= \nu \frac{\partial^2 w^1_{(k)}}{\partial x_2 \partial x_2} + R_{1k}, \\ \sum_{m=0}^{k} \left\{ w^1_{(m)} \frac{\partial w^3_{(k-m)}}{\partial x_1} + w^2_{(m)} \frac{\partial w^3_{(k-m)}}{\partial x_2} + w^3_{(m)} \frac{\partial w^3_{(k-m)}}{\partial x_3} \right. &= \nu \frac{\partial^2 w^3_{(k)}}{\partial x_2 \partial x_2} + R_{3k}, \\ \partial w^1_{(k)}/\partial x_1 + \partial w^2_{(k)}/\partial x_2 &= Q_k, \end{aligned}\right\} \tag{27}$$

where

$$R_{10} = R_{11} = 0, \quad R_{12} = 2\omega w^3_{(1)} + x_1(\omega)^2, \quad R_{13} = 2\omega w^3_{(2)},$$

$$R_{14} = 2\omega w^3_{(3)} - \frac{w^3_{(1)}}{(x_3)^2}\frac{(U)^2}{\omega} - \frac{x_1}{(x_3)^2}(U)^2, \quad R_{15} = 2\omega w^3_{(4)} - \frac{w^3_{(2)}}{(x_3)^2}\frac{(U)^2}{\omega}, \ldots,$$

$$R_{31} = -2\omega w^1_{(0)} + x_3(\omega)^2, \quad R_{32} = -2\omega w^1_{(1)},$$

$$R_{33} = -2\omega w^1_{(2)} + \frac{2w^1_{(0)}}{(x_3)^2}\frac{(U)^2}{\omega}, \quad R_{34} = -2\omega w^1_{(3)} + \frac{w^1_{(1)}}{(x_3)^2}\frac{(U)^2}{\omega}, \ldots,$$

$$Q_0 = Q_1 = 0, \quad Q_2 = -\partial w^3_{(1)}/\partial x_3, \quad Q_3 = -\partial w^3_{(2)}/\partial x_3,$$

$$Q_4 = -\frac{\partial w^3_{(3)}}{\partial x_3} - \frac{x_1}{(x_3)^4}\left(\frac{U}{\omega}\right)^2 w^1_{(0)}, \quad Q_5 = -\frac{\partial w^3_{(4)}}{\partial x_3} - \frac{x_1}{(x_3)^4} w^1_{(1)}, \ldots.$$

The mainstream flow is expanded in the similar manner:

$$\left.\begin{aligned}\frac{W^1}{x_3\omega} &= 1+\frac{1}{2}\left(\frac{x_1}{x_3}\right)^2\left(\frac{\beta}{x_1}\right)^2-\frac{1}{8}\left(\frac{x_1}{x_3}\right)^4\left(\frac{\beta}{x_1}\right)^4+\dots,\\ \frac{W^3}{x_3\omega} &= -\left[\frac{x_1}{x_3}-\frac{1}{2}\left(\frac{x_1}{x_3}\right)^3\left(\frac{\beta}{x_1}\right)^2+\left(\frac{x_1}{x_3}\right)^5\left\{\frac{3}{8}\left(\frac{\beta}{x_1}\right)^4-\left(\frac{\beta}{x_1}\right)^2\right\}+\dots\right],\end{aligned}\right\} \tag{28}$$

where $\beta = U/\omega$, which gives the following boundary conditions for $w^i_{(k)}$:

$$\left.\begin{aligned}&w^1_{(k)} = w^2_{(k)} = w^3_{(k)} = 0 \quad \text{at} \quad x_2 = 0,\\ &\left.\begin{aligned}\tilde{w}^1_{(0)}\to 1,\quad \tilde{w}^1_{(1)}\to 0,\quad \tilde{w}^1_{(2)}\to \tfrac{1}{2}(\beta/x_1)^2,\dots\\ \tilde{w}^3_{(1)}\to 1,\quad \tilde{w}^3_{(2)}\to 0,\quad \tilde{w}^3_{(3)}\to -\tfrac{1}{2}(\beta/x_1)^2,\dots\end{aligned}\right\} \text{ as } \quad x_2\to\infty.\end{aligned}\right\} \tag{29}$$

To solve this system of equations, the independent variable x_2 is transformed to η according to

$$\eta = x_2(x_3\omega/\nu x_1)^{\frac{1}{2}} \tag{30}$$

and the $w^i_{(k)}$ are divided into terms composed of similar functions as follows:

$$\left.\begin{aligned}w^1_{(k)} &= (x_1/x_3)^k\{u^{(k)}_0(\eta)+(\beta/x_1)^2 u^{(k)}_2(\eta)+\dots+(\beta/x_1)^m u^{(k)}_m(\eta)\},\\ w^2_{(k)} &= (x_1/x_3)^k\{v^{(k)}_0(\eta)+(\beta/x_1)^2 v^{(k)}_2(\eta)+\dots+(\beta/x_1)^m v^{(k)}_m(\eta)\},\\ w^3_{(k)} &= (x_1/x_3)^k\{w^{(k)}_1(\eta)+(\beta/x_1)^2 w^{(k)}_3(\eta)+\dots+(\beta/x_1)^m w^{(k)}_{m+1}(\eta)\},\end{aligned}\right\} \tag{31}$$

where $m = k$ or $k-1$, whichever is an even integer, and $w^3_{(0)} = 0$.

For $k = 0$, the stream function $\psi^{(0)}$ is introduced so as to satisfy the zero-order equation of continuity, namely,

$$u^{(0)}_0 = \frac{\partial\psi^{(0)}}{\partial x_2}, \quad v^{(0)}_0 = -\left(\frac{x_1x_3\omega}{\nu}\right)^{\frac{1}{2}}\frac{\partial\psi^{(0)}}{\partial x_1}.$$

Substitution of $\psi^{(0)} = (\nu x_1/\omega x_3)^{\frac{1}{2}} f_0(\eta)$ into (27) yields

$$\left.\begin{aligned}&2f'''_0+f_0f''_0 = 0,\\ &f_0(0) = f'_0(0) = 0, \quad f'_0(\infty)\to 1,\end{aligned}\right\} \tag{32}$$

where a prime indicates a derivative with respect to η. $f_0(\eta)$ is the well-known function representing the laminar boundary layer along a flat plate, namely, Blasius flow.

For $k = 1$, the stream function $\psi^{(1)}$ related to $u^{(1)}_0$ and $v^{(1)}_0$ by

$$u^{(1)}_0 = \frac{1}{x_1}\frac{\partial\psi^{(1)}}{\partial x_2}, \quad v^{(1)}_0 = -\frac{1}{x_1}\left(\frac{x_1x_3\omega}{\nu}\right)^{\frac{1}{2}}\frac{\partial\psi^{(1)}}{\partial x_1}$$

satisfies the first-order equation of continuity. Substitution of

$$\psi^{(1)} = x_1\left(\frac{\nu x_1}{\omega x_3}\right)^{\frac{1}{2}} f_1(\eta)$$

into (27) gives

$$\left.\begin{aligned}&2f'''_1+f_0f''_1-2f'_0f'_1+3f''_0f_1 = 0,\\ &f_1(0) = f'_1(0) = 0, \quad f'_1(\infty)\to 0,\end{aligned}\right\} \tag{33}$$

which gives the solution $f_1(\eta) \equiv 0$. For the first-order cross-flow, (27) and (28) give

$$\left.\begin{aligned} 2g_1''' + f_0 g_1'' - 2f_0' g_1'' &= 2(2f_0' - 1), \\ g_1(0) = g_1'(0) = 0, \quad g_1'(\infty) &= -1, \end{aligned}\right\} \tag{34}$$

in which $w_1^{(1)} = g_1'(\eta)$.

The zero-order solution gives the flow only in the x_1 direction and the first-order solution gives the cross-flow that corresponds to the zero-order x_1-wise flow. Similarly, at higher order, even-order solutions give higher-order modifying flows only in the x_1 direction and the odd-order solutions give the higher-order cross-flows corresponding to the x_1-wise flows that are one order lower than themselves. $f_0(\eta)$ and $g_1(\eta)$ are the lowest pair of this infinite set and contain no influence of three-dimensionality of the blade neither in the equations themselves nor in the boundary conditions. These flows are the ones given by Fogarty and also the first two terms of Tan's solution.

For $k = 2$, $w_{(2)}^3 = 0$, and two stream functions $\psi_0^{(2)}$ and $\psi_2^{(2)}$ defined by

$$u_0^{(2)} = \frac{1}{(x_1)^2}\frac{\partial \psi_0^{(2)}}{\partial x_2}, \quad v_0^{(2)} = -\left(\frac{x_1 x_3 \omega}{\nu}\right)^{\frac{1}{2}} \frac{1}{(x_1)^2}\frac{\partial \psi_2^{(2)}}{\partial x_1} - \tfrac{1}{2}(\eta g_1' - g_1), \quad u_2^{(2)} = \frac{\partial \psi_2^{(2)}}{\partial x_2},$$

$$v_2^{(2)} = -\left(\frac{x_1 x_3 \omega}{\nu}\right)^{\frac{1}{2}} \frac{\partial \psi_2^{(2)}}{\partial x_1}$$

are introduced so as to satisfy the second-order equation of continuity. Putting

$$\psi_0^{(2)} = (x_1)^2 \left(\frac{\nu x_1}{\omega x_3}\right)^{\frac{1}{2}} f_{20}(\eta), \quad \psi_2^{(2)} = \left(\frac{\nu x_1}{\omega x_3}\right)^{\frac{1}{2}} f_{22}(\eta)$$

and substituting them into the second-order equations of (27), one gets the following differential equations and boundary conditions for the similar functions $f_{20}(\eta)$ and $f_{22}(\eta)$:

$$\left.\begin{aligned} 2f_{20}''' + f_0 f_{20}'' - 4f_0' f_{20}' + 5f_{20}'' f_0 &= f_0'' g_1 - 4g_1' - 2 + 2f_0' g_1', \\ f_{20}(0) = f_{20}'(0) = 0, \quad f_{20}'(\infty) &\to 0, \end{aligned}\right\} \tag{35}$$

$$\left.\begin{aligned} 2f_{22}''' + f_0 f_{22}'' + f_{22} f_0'' &= 0, \\ f_{22}(0) = f_{22}'(0) = 0, \quad f_{22}'(\infty) &\to \tfrac{1}{2}. \end{aligned}\right\} \tag{36}$$

Then,

$$u_0^{(2)} = f_{20}'(\eta), \quad u_2^{(2)} = f_{22}'(\eta).$$

For $k = 3$, $w_{(3)}^1 = w_{(3)}^2 = 0$ and the third-order cross-flows represented by similar functions $w_1^{(3)} = g_{30}'(\eta)$ and $w_3^{(3)} = g_{33}'(\eta)$ are obtained from the solution of

$$\left.\begin{aligned} 2g_{30}''' + f_0 g_{30}'' - 6f_0' g_{30}' &= -5f_{20} g_1'' + 2f_{20}' g_1' + 4f_{20}' + g_1 g_1'', \\ g_{30}(0) = g_{30}'(0) = 0, \quad g_{30}'(\infty) &\to 0, \end{aligned}\right\} \tag{37}$$

$$\left.\begin{aligned} 2g_{33}'' + f_0 g_{33}'' - 2f_0' g_{33}' &= -f_{22} g_1'' + 2f_{22}' g_1' + 4f_{22}' - 2f_0', \\ g_{33}(0) = g_{33}'(0) = 0, \quad g_{33}'(\infty) &\to \tfrac{1}{2}. \end{aligned}\right\} \tag{38}$$

The higher-order flows are obtained by exactly the same operations as those used above to reduce the partial differential equations (27) to a set of ordinary ones, for each order of flow.

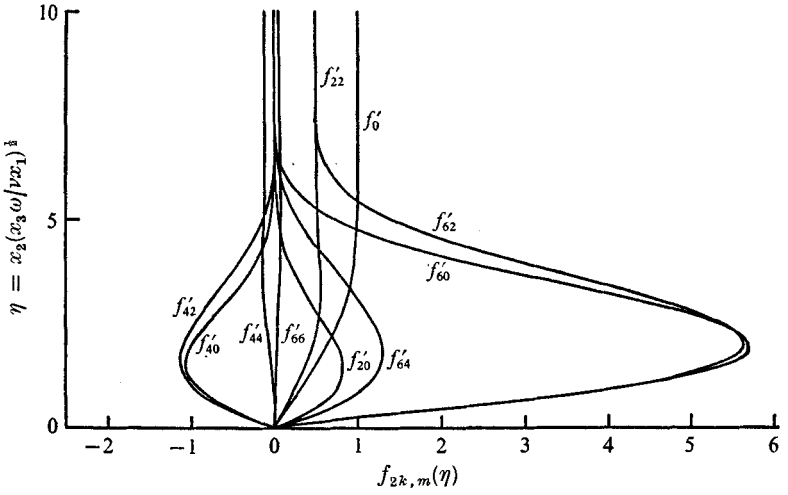

FIGURE 2. Functions $f_{2k,m}(\eta)$.

The resulting contravariant velocities w^1 and w^3 are expressed in terms of $f_{kl}(\eta)$ and $g_{mn}(\eta)$, according to

$$\left.\begin{aligned} w^1/x_3\omega &= f'_0(\eta) + (x_1/x_3)^2\{f'_{20}(\eta) + (\beta/x_1)^2 f'_{22}(\eta)\} \\ &\quad + (x_1/x_3)^4\{f'_{40}(\eta) + (\beta/x_1)^2 f'_{42}(\eta) + (\beta/x_1)^4 f'_{44}(\eta)\} + \ldots, \\ w^3/x_3\omega &= (x_1/x_3)\, g'_1(\eta) + (x_1/x_3)^3\{g'_{31}(\eta) + (\beta/x_1)^2 g'_{33}(\eta)\} \\ &\quad + (x_1/x_3)^5\{g'_{51}(\eta) + (\beta/x_1)^2 g'_{53}(\eta) + (\beta/x_1)^4 f'_{55}(\eta)\} + \ldots. \end{aligned}\right\} \tag{39}$$

These contravariant velocities are transformed into physical ones by

$$\hat{w}_1 = w^1, \quad \hat{w}_3 = \{1 + (x_1/x_3)^2 \sin^2\phi \cos^2\phi\}^{\frac{1}{2}} w^3. \tag{40}$$

Among the similar functions introduced above, $g_1(\eta)$ was numerically computed by Fogarty and $f_{20}(\eta)$ by McCrosky & Yaggy. The functions whose second subscript is zero, such as $f_{20}(\eta), f_{40}(\eta), \ldots$, and those whose second subscript is 1, such as $g_{31}(\eta), g_{51}(\eta), \ldots$, are sufficient to express the flow in the case $\phi = 0$, i.e. a rotating flat plate. Other newly introduced similar functions are used to express the influence of three-dimensionality of the blade.

$f_{kl}(\eta)$ and $g_{mn}(\eta)$ were computed numerically using the Runge–Kutta method on a digital computer with an integration step $\Delta\eta = 0{\cdot}005$ and are shown in figures 2 and 3.

7. The boundary-layer flow along a blade element

The velocity components given by (39) and (40) are the components in the directions of curvilinear co-ordinate axes, though physical ones. But the flow is more clearly understood in terms of two components in the directions of the main-flow streamline (chordwise component) and the cross-flow on the blade surface, perpendicular to the main-flow direction (spanwise component).

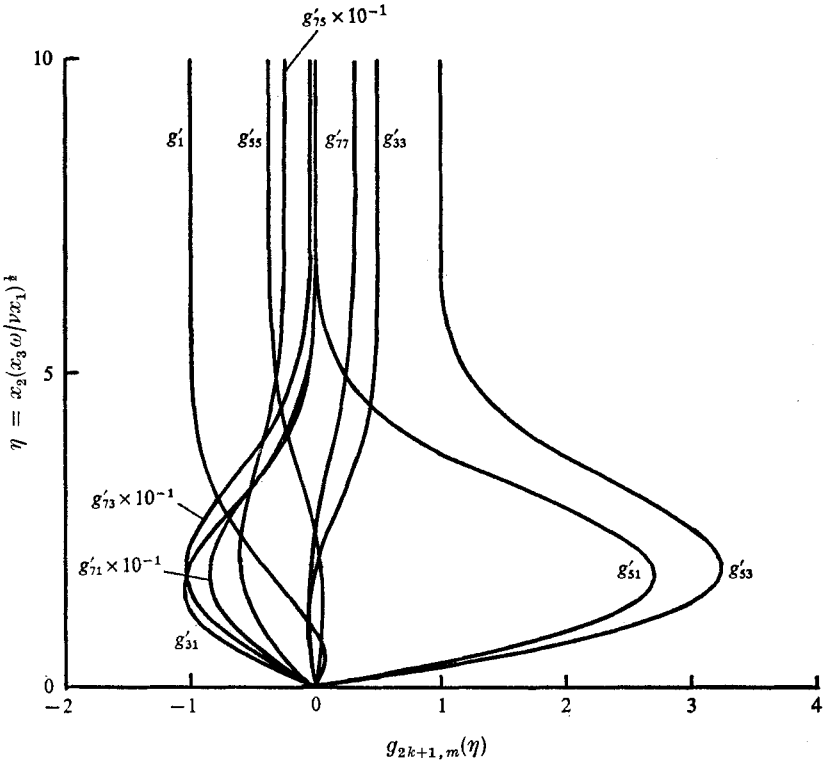

FIGURE 3. Functions $g_{2k+1,m}(\eta)$.

The direction cosines of a chordwise unit vector are given by (20) and those of a spanwise unit vector are given by

$$l_s = \frac{x_1\cos\phi}{\{(x_3)^2+(x_1)^2\cos^2\phi\}^{\frac{1}{2}}}, \quad m_s = 0, \quad n_s = \frac{x_3}{\{(x_3)^2+(x_1)^2\cos^2\phi\}^{\frac{1}{2}}}. \tag{41}$$

These values enable one to calculate chordwise and spanwise physical components of the flow from $\hat{w}_1$ and $\hat{w}_3$ according to

$$\hat{w}_c = (l_T l_1 + m_T m_1 + n_T n_1)\hat{w}_1 + (l_T l_3 + m_T m_3 + n_T n_3)\hat{w}_3,$$
$$\hat{w}_s = (l_s l_1 + m_s m_1)\hat{w}_1 + (l_s l_3 + m_s m_1)\hat{w}_3.$$

The magnitude $\hat{W}$ of the mainstream flow given by (21) is assumed here to be constant along a blade element and the non-dimensional forms of $\hat{w}_c$ and $\hat{w}_s$ divided by $\hat{W}$ are

$$\left.\begin{aligned}\frac{\hat{w}_c}{\hat{W}} &= \frac{1}{\{(r/x_3)^2+(U/\omega x_3)^2\}^{\frac{1}{2}}}\left(\frac{(S)^2}{T}\frac{\hat{w}_1}{x_3\omega} - \frac{x_1 S\cos^2\phi}{T}\frac{\hat{w}_3}{x_3\omega}\right),\\ \frac{\hat{w}_s}{\hat{W}} &= \frac{1}{\{(r/x_3)^2+(U/\omega x_3)^2\}^{\frac{1}{2}}}\left[\frac{x_1\cos^2\phi}{\{(x_3)^2+(x_1)^2\cos^2\phi\}^{\frac{1}{2}}}\frac{\hat{w}_1}{x_3\omega} + \frac{S}{\{(x_3)^2+(x_1)^2\cos^2\phi\}^{\frac{1}{2}}}\frac{\hat{w}_3}{x_3\omega}\right].\end{aligned}\right\} \tag{42}$$

In the above equations, x_1 and x_3 are not independent but related by

$$(x_1)^2 \cos^2\phi + (x_3)^2 = r^2, \tag{43}$$

where r is constant for the blade element under consideration and ϕ must satisfy the relation (3). x_1 designates a co-ordinate of a point on the blade element considered but is not a real distance from the leading edge along the blade element. In fact, the real length l is given by

$$l = \int_0^{x_1} \{1 - (x_1/r)^2 \cos^4\phi\}^{-\frac{1}{2}} dx_1. \tag{44}$$

The wall friction stress τ_C in the chordwise direction is expressed as a non-dimensional coefficient C_{fc} times $\frac{1}{2}\rho(\hat{W})^2$ as follows:

$$C_{fc} = \frac{\tau_c}{\frac{1}{2}\rho(\hat{W})^2} = \frac{2}{Re^{\frac{1}{2}}} \left(\frac{l}{x_1}\right)^{\frac{1}{2}} \left(\frac{x_3}{r}\cos\phi_0\right)^{\frac{3}{2}} \left[\frac{(S)^2}{T}\tau_1 - \frac{x_1 S\cos\phi}{T}\tau_3\right], \tag{45}$$

where $Re = \hat{W}l/\nu$, ϕ_0 is the value of ϕ at the leading edge of the blade element considered, i.e. $\tan\phi_0 = U/\omega r$, and τ_1 and τ_3 are calculated in terms of the second derivatives of the similar functions as follows:

$$\begin{aligned}
\tau_1 &= f_0''(0) + (x_1/x_3)^2\{f_{20}''(0) + (\beta/x_1)^2 f_{22}''(0)\} \\
&\quad + (x_1/x_3)^4\{f_{40}''(0) + (\beta/x_1)^2 f_{42}''(0) + (\beta/x_1)^4 f_{44}''(0)\} + \ldots, \\
\tau_3 &= (x_1/x_3)[g_1''(0) + (x_1/x_3)^2\{g_{31}''(0) + (\beta/x_1)^2 g_{33}''(0)\} \\
&\quad + (x_1/x_3)^4\{g_{51}''(0) + (\beta/x_1)^2 g_{53}''(0) + (\beta/x_1)^4 g_{55}''(0)\} + \ldots].
\end{aligned}$$

8. Results and discussion

The solution given above is presented in the form of series expansions in terms of two parameters x_1/x_3 and β/x_3, both of which restrict the convergence of the series. The wall stress coefficient, for which the derivatives of velocity variations at the wall are responsible, is especially difficult to obtain with sufficient accuracy for large values of these two parameters; the restriction on x_1/x_3, in particular, being severe. In a discussion with emphasis on the influence purely of three-dimensionality of the blade configuration, the results for which the contributions of terms higher than $(x_1/x_3)^4$ are sufficiently small are useful, and are shown below.

Figures 4 and 5 show chordwise and spanwise velocity distributions in the boundary layer along some main-flow streamlines. The ordinate η^* represents the distance from the wall and is related to the argument η of aforementioned similar functions as follows:

$$\eta^* = \eta\left(\frac{x_1}{l}\right)^{\frac{1}{2}} \left\{1 + \left(\frac{r}{x_3}\right)^2 \tan^2\phi_0\right\}^{\frac{1}{2}}. \tag{46}$$

The spanwise cross-flow grows almost linearly with distance from the leading edge, where only the chordwise stream exists for any value of stagger angle ϕ_0. This chordwise velocity at the leading edge is given in series form as

$$\hat{w}_c/\hat{W} = \cos\phi_0\{f_0'(\eta) + \tan^2(\phi_0) f_{22}'(\eta) + \tan^4(\phi_0) f_{44}'(\eta) + \ldots\} \tag{47}$$

and is identical to that of the well-known Blasius flat-plate boundary-layer flow.

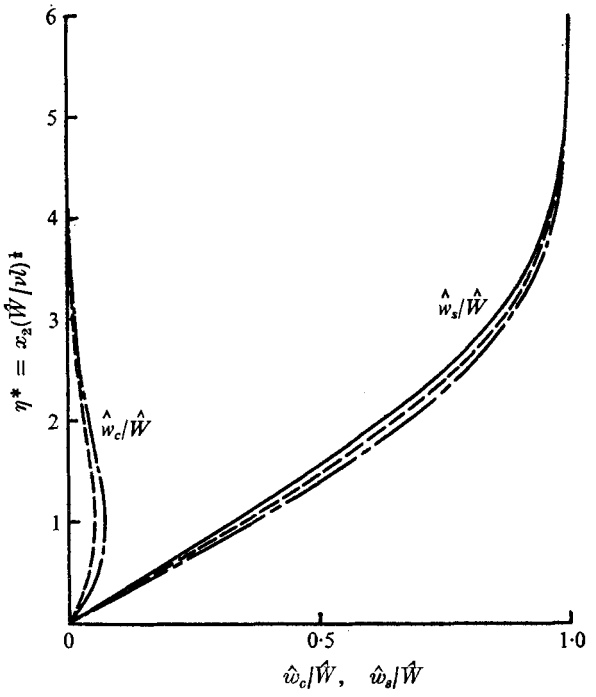

FIGURE 4. Chordwise ($\hat{w}_c/\hat{W}$) and spanwise ($\hat{w}_s/\hat{W}$) velocity profiles in the boundary layer for various downstream positions; $\phi_0 = \tan^{-1}(0{\cdot}2)$. ——, $l/r = 0$ (also Blasius flow and Horlock & Wordsworth's results); — — —, $l/r = 0{\cdot}2$; —·—, $l/r = 0{\cdot}3$; $\hat{w}_c/\hat{W} = 0$ for $l/r = 0$.

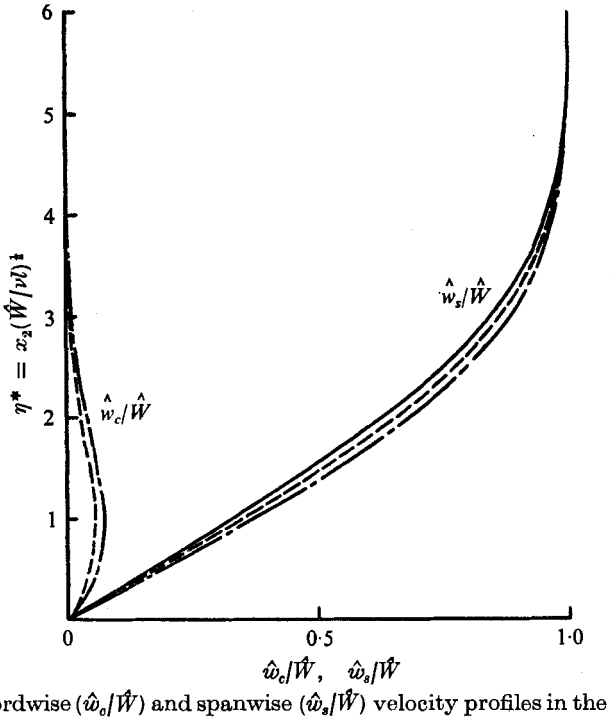

FIGURE 5. Chordwise ($\hat{w}_c/\hat{W}$) and spanwise ($\hat{w}_s/\hat{W}$) velocity profiles in the boundary layer for various blade angles; $l/r = 0{\cdot}2$. ——, Blasius flow; —·—, $\phi_0 = 0$; — — —, $\phi_0 = \tan^{-1}(0, 2)$.

The case $\phi_0 = 0$ corresponds to a rotating flat plate, for which earlier results of Fogarty (1951), Tan (1953) and McCrosky & Yaggy (1968) are available. The curves for $\phi_0 = 0$ are coincident with Tan's solution in principle, i.e. the functions except for f_0, f_{20} and g_1 had to be recalculated, because Tan gave only the equations that f_0, f_{k0}, g_1 and $g_{k+1,1}$ must satisfy, and not the numerical values. Fogarty used only f_0 and g_1 to express the chordwise and spanwise velocities and the solution for pure hovering motion in the special case of a helicopter rotor blade presented by McCrosky & Yaggy adopts only f_0, f_{20} and g_1; hence, these two solutions are less accurate than Tan's solution for the present problem.

The cases $\phi \neq 0$ are the ones newly treated in this work and for these the study of Horlock & Wordsworth (1965) is available for comparison. They analysed a laminar boundary layer on a rotating thin helical blade of both a turbine and a compressor rotor to formulate successfully the effect of stagger. In that solution, a mainflow streamline is assumed to be the intersection of the blade and a circular cylinder whose centre-line is the rotating axis and the magnitude of the mainflow velocity is constant along these streamlines. These assumptions are the same as those of the present study, but in Horlock & Wordsworth's solution, the blade angle is assumed to be constant at any point on the blade surface and, correspondingly, the upstream flow approaching the rotor is not uniform. This particular approaching flow permits the thin helical blade to have similar velocity fields in the boundary layer both in the chordwise and spanwise directions. Figures 4 and 5 demonstrate that the chordwise velocity distribution varies with both stagger angle and distance from the leading edge, contrary to the prediction of Horlock & Wordsworth. In the present study, a more practical blade configuration and approaching flow are adopted and this makes the boundary-layer flow unequilibrated locally. It must be noted that the growth of secondary flow induces the higher rate of entrainment of main-flow fluid of higher energy, causing the higher resistance to boundary-layer separation, compared with Blasius flat-plate flow. In figure 4, which shows the dependence on distance from the leading edge, the secondary cross-flow grows in the downstream direction and in figure 5, which demonstrates the effect of stagger, the secondary flow grows more rapidly in cases where the inclination of a blade element to the axial flow direction is larger. In both cases, the flatter chordwise velocity distribution corresponds to the stronger secondary flow. By the way, in figure 5, the case $\tan\phi_0 = \infty$ corresponds to either $\omega = 0$ or $r = 0$, both of which coincide with Blasius flow.

The chordwise wall shear stress expressed in the form of the coefficient $C_f Re^{\frac{1}{2}}$ exhibits larger values for smaller ϕ_0 and larger l/r, as shown in figure 6. This is another way of stating the above-mentioned fact. At the leading edge, $C_f Re^{\frac{1}{2}}$ takes the well-known value for the flat-plate case, i.e. 0·664. Figure 6 indicates that when one considers a blade element on one specified cylindrical flow surface, a more inclined blade element, namely, one designed for a relatively larger rotating speed compared with the axial flow velocity, exhibits a larger wall shear stress, increasing nearer to the trailing edge. But this does not mean immediately that the blade tip is more advantageous than the root in regard to boundary-layer separation. On the contrary, if one compares the wall shear stress at stations some distance away from the leading edge on different blade elements of one

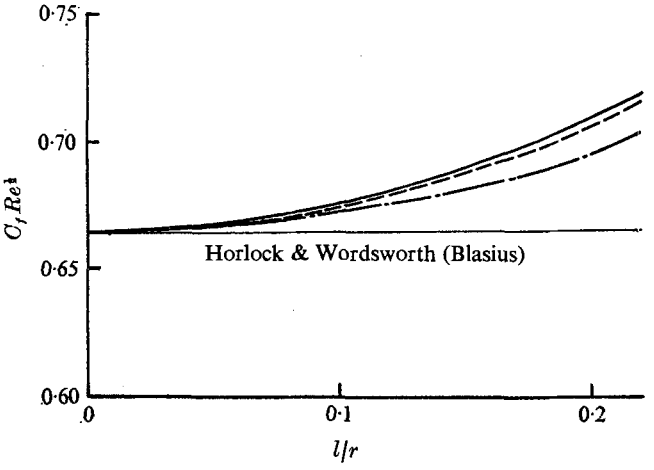

FIGURE 6. Downstream variation of wall stress coefficient $C_f Re^{\frac{1}{2}}$ with blade angle ϕ_0. ——, $\phi_0 = 0$; – – –, $\phi_0 = \tan^{-1}(0{\cdot}2)$; —·—, $\phi_0 = \tan^{-1}(0{\cdot}3)$; ——, Horlock & Wordsworth (also Blasius flow).

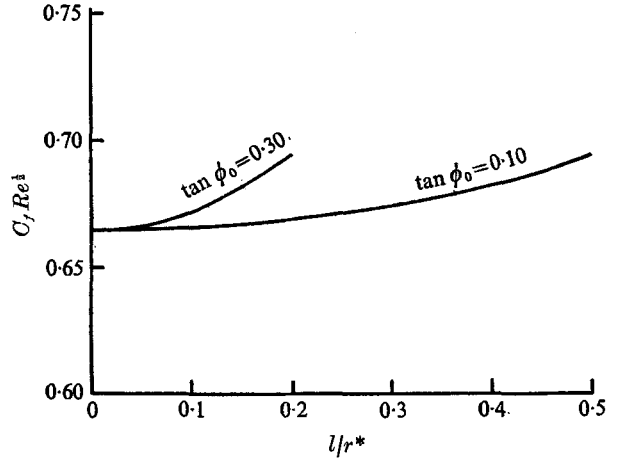

FIGURE 7. Comparison of wall shear stress coefficient on two blade elements at the stations the same distance apart from the leading edge. r^* is the radius of the flow surface for which $\phi_0 = \tan^{-1}(0{\cdot}10)$.

particular blade, one finds that the blade element nearer to the hub exhibits a larger $C_f Re^{\frac{1}{2}}$ value, as shown in figure 7, in which the downstreamwise variations of the wall shear stress coefficient along two blade elements having $\phi_0 = \tan^{-1}(0{\cdot}1)$ and $\phi_0 = \tan^{-1}(0{\cdot}3)$ are shown, the abscissa being l/r^* and not l/r, where r^* is the distance from the rotating axis of the blade element for $\phi_0 = \tan^{-1}(0{\cdot}1)$.

As for the cross-flow, Horlock & Wordswoth give the following equation, for a compressor rotor blade with prerotation in the approaching flow:

$$\hat{w}_s/\hat{W} = (l/r)\cos^2\phi_i\{g(\eta^*) - h(\eta^*)\}, \tag{48}$$

where ϕ_i is the blade angle and $g(\eta^*)$ and $h(\eta^*)$ are functions only of η^*. This equation shows that the cross-flow velocity distribution is also similar although

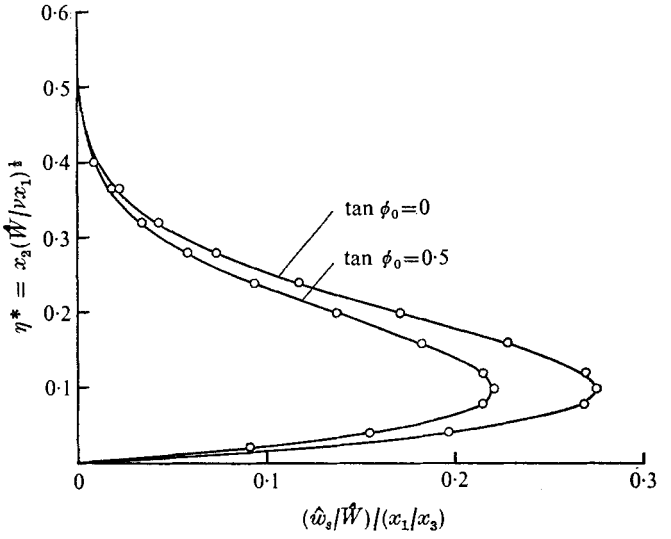

FIGURE 8. The cross-flow velocity profile in the boundary layer at the leading edge. ○, Horlock & Wordsworth; ——, present analysis.

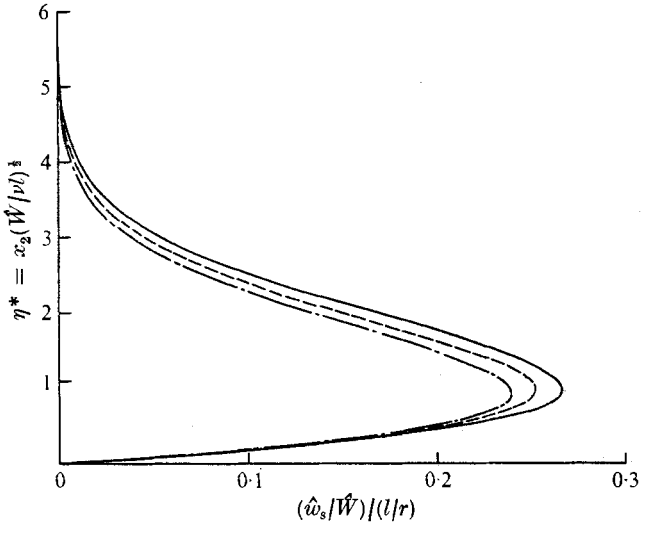

FIGURE 9. Collapsed cross-flow velocity profiles for various downstream positions from the leading edge; $\phi_0 = \tan^{-1}(0{\cdot}2)$. ——, $l/r = 0$; – – –, $l/r = 0{\cdot}2$; —· —, $l/r = 0{\cdot}3$. The curve for $l/r = 0$ is also that from Horlock & Wordsworth.

the magnitude depends on ϕ_i and l/r. The difference between the blade configurations of Horlock & Wordsworth and the present analysis makes direct comparison of (42) and (48) impossible, but in the limit $x_1 \to 0$, or at the leading edge, the blade configurations become identical. Then (42) becomes

$$\lim_{x_1 \to 0} (\hat{w}_s/\hat{W}) = (x_1/r)\,[\cos^3\phi_0\{f_0'(\eta) + \tan^2\phi_0 f_{22}'(\eta) + \tan^4\phi_0 f_{44}'(\eta) + \ldots\} + \cos^2\phi_0\{g_1'(\eta) + \tan^2\phi_0 g_{33}'(\eta) + \tan^4\phi_0 g_{55}'(\eta) + \ldots\}], \quad (49)$$

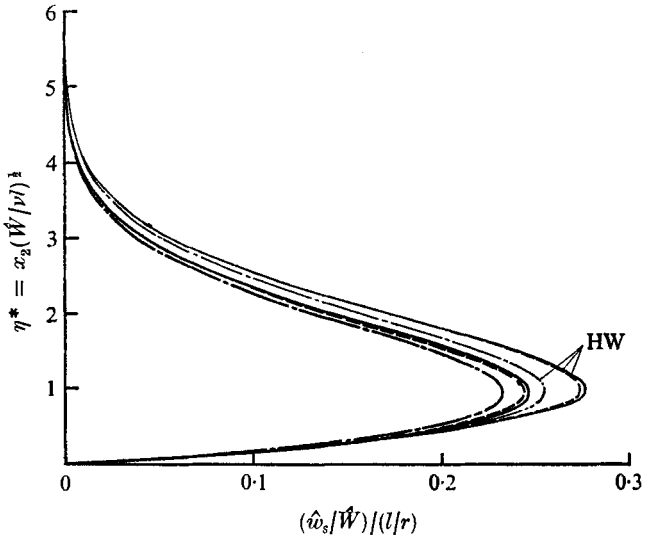

FIGURE 10. Collapsed cross-flow velocity profiles for various blade angles; $l/r = 0{\cdot}2$. ——, $\phi_0 = 0$; – – –, $\phi_0 = \tan^{-1}(0{\cdot}1)$; —·—, $\phi_0 = \tan^{-1}(0{\cdot}2)$. HW, Horlock & Wordsworth.

and (48) remains unchanged. These two are different with respect to not only the functions employed but also the independent variable. However, after transforming the independent variable according to $\eta^* = \eta/\cos^{\frac{1}{2}}\phi_0$, which holds at the leading edge, one finds that the two solutions agree well as shown in figure 8. The details of the cross-flow velocity distribution are given in figures 9 and 10: downstream variation for a particular blade angle in figure 9 and dependence on the blade angle ϕ_0 in figure 10. The curves labelled HW were computed from (48) and the unlabelled curve for $\phi_0 = 0$ is also Tan's solution. The cross-flow also exhibits non-similarity as the counterpart of a non-similar flow field in chordwise boundary-layer flow. However, (48), given by Horlock & Wordsworth, turns out to be a good approximation for the evaluation of the growth rate of cross-flow, though exaggerating it a little.

Blasius flow is an equilibrium flow in the sense that similarity exists. The analysis of Horlock & Wordsworth is based on the assumption that the rotating-blade boundary-layer flow can be approximated by an equilibrium flow. The present analysis indicates that the spanwise cross-flow growth does not prevent retention of the equilibrium and acts favourably with regard to the separation of the boundary-layer flow.

9. Conclusions

The present analysis investigates the influence of the three-dimensionality of a rotating blade in a uniform axial flow on the laminar boundary layer which develops from the leading edge on its surface. The equation of the flow, which is the starting point of the analysis, is deduced very clearly for a complicated three-dimensional blade by transforming the equations of motion for a rotating system in vector form into tensor form. This way of deriving the basic equations is

applicable to any other kind of blade configuration. The blade configuration selected in the analysis is a rather practical one and it gives, together with the assumed simple mainstream flow, the general features of boundary-layer flow on a three-dimensional blade.

The authors wish to express their sincere gratitude to Prof. S. Murata of Osaka University, who has had many encouraging and stimulating discussions with them throughout this work.

REFERENCES

BOGDANOVA, V. V. 1971 *Mekh. Zhid. i Gaza*, no. 2, p. 84.
FOGARTY, L. E. 1951 *J. Aero. Sci.* **18**, 247.
HORLOCK, J. H. & WORDSWORTH, J. 1965 *J. Fluid Mech.* **23**, 305.
MCCROSKY, W. J. & YAGGY, P. F. 1968 *A.I.A.A. J.* **6**, 1919.
TAKEMATSU, M. 1972 *A.I.A.A. J.* **10**, 333.
TAN, H. S. 1953 *J. Aero. Sci.* **20**, 780.
TOYOKURA, T. & HARADA, K. 1969 *J. Japan. Soc. Mech. Engrs*, **72**, 56 (in Japanese).